Simulation of Buckling and Post-Buckling Behavior of Structures Using Applied Element Method

by

Kimiro Meguro* **and Hatem Tagel-Din****

ABSTRACT

A new extension for the Applied Element Method (AEM) for structural analysis is introduced. This paper deals with the large deformation of elastic structures under static loading condition. In the formulation used, no geometric stiffness matrix is adopted. The formulation used is simple and general and it can be applied for any structural configuration or material type. This technique is based on determination of the residual forces due to geometrical changes of the structure during simulation. The accuracy of the proposed technique is checked by comparing with the theoretical results and, in all cases, the buckling loads, mode and post-buckling behavior of structures can be followed accurately.

INTRODUCTION

Structural behavior is divided, from numerical point of view, into small and large deformation analysis. In small deformation range, the changes of the structure geometry during loading is neglected. Buckling of columns, which is one of main reason of failure of slender columns, can be detected only using large deformation theory. Many numerical analysis were performed for large deformation stage using the FEM[1), 2), 3)]. Using the FEM, buckling mode, load and post buckling behavior can be followed. Unfortunately, FEM assumes that material is continuum and special techniques should be adopted to consider separation between structural members. As the fracture plan in most of cases, especially concrete structures, is arbitrary and it can not be defined before analysis, representation of separation by joint elements makes the method lose the reliability required for failure analysis. However, it is very difficult to deal with geometrical changes together with separation problems using FEM, especially if the studied region is a potentially highly damaged material like bricks or reinforced concrete. These complications makes the applicability of these methods limited for large deformation and collapse behavior of steel structures, where the material is continuum.

One of the recent methods to deal with failure analysis of structures is the Modified or Extended Distinct Element Method, (MDEM[4)] or EDEM[5)]). This method can follow the highly non-linear geometric changes of the structure during failure, however, the main disadvantages of this method are that in some cases accuracy is not enough for quantitative discussion and it needs relatively long CPU time compared with the FEM. In addition, the accuracy of the EDEM was not checked in case of buckling of elastic structures. The applicability of other methods adopting rigid elements, like Rigid Body and Spring Model RBSM[6), 7)], were not verified in case of buckling of structures. Other methods like Discontinuous Deformation Analysis, DDA[8)], were applied for large deformation of rocks. The DDA applicability is still limited to behavior of rocks or bricks...etc, which are initially separated.

The proposed method, termed Applied Element Method (AEM) is based on dividing the structural members into virtual elements. Each element totally represents stresses, strains, deformations and failure of a

* Associate Professor, International Center for Disaster-Mitigation Engineering, Institute of Industrial Science, The University of Tokyo
** Ph.D., visiting researcher, Institute of Industrial Science, The University of Tokyo

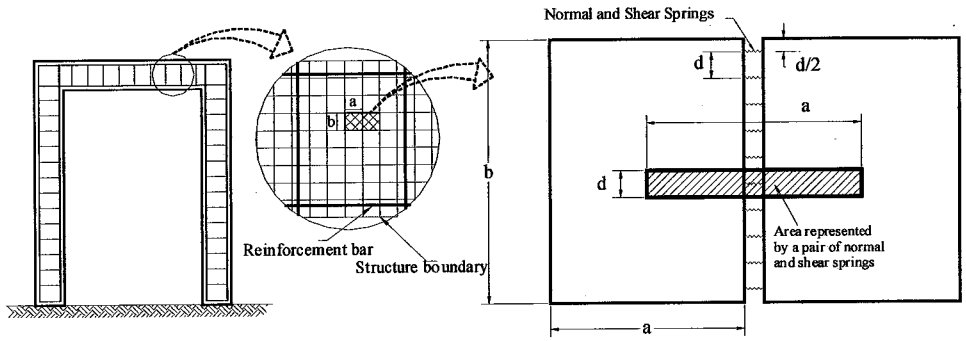

(a) Element generation for AEM (b) Spring distribution and area of influence of each pair of springs

Fig. (1) Modelling of structure to AEM

certain area. The accuracy of the AEM in small deformation range was checked in Ref. (9) and (10). It was proved[9] that the AEM can follow internal stresses and strain and crack initiation, location and propagation. In addition, the load-displacement relation and the failure load can be calculated with reasonable accuracy. The complicated process of crack opening and closing in cyclic loading analysis can also be followed[9]. Even the, conventionally neglected, effects of Poisson's ratio could be considered accurately[10]. It was proved also that the simulation results do not heavily depend on the element shape or arrangement, like in case or EDEM and RBSM[11]. The applicability of the method to follow rigid body motion of failed structural elements was checked in Ref. (12).

This paper introduces a new extension for the AEM for buckling and post-buckling behavior of structures. For quantitative discussion, analyses were performed for elastic structures to compare the accuracy with the theoretical results. It is proved through comparison with theoretical results that, using the AEM, the calculated buckling loads, buckling modes and load-displacement relations agree well with the theoretical results.

SMALL DEFORMATION SIMULATION

With the AEM, structure is modelled as an assembly of small elements which are made by dividing of the structure virtually, as shown in Fig. (1) (a). The two elements shown in Fig. (1) are assumed to be connected by pairs of normal and shear springs located at contact points which are distributed around the element edges. Each pair of springs totally represent stresses and deformations of a certain area (hatched area in Fig. 1 (b)) of the studied elements. Referring to Eq.(1), the spring stiffness is determined as:

$$K_n = \frac{E*d*T}{a} \text{ and } K_s = \frac{G*d*T}{a} \quad (1)$$

Where, d is the distance between springs, T is the thickness of the element and "a" is the length of the representative area, E and G are the Young's and shear modulus of the material, respectively. The above equation indicates that each spring represents the stiffness of an area (d*T) with length "a" of the studied material. In case of reinforcement, this area is replaced by that of the reinforcement bar. The above equation indicates that the spring stiffness is calculated as if the spring connects the element centerlines.

Three degrees of freedom are assumed for each element. These degrees of freedom represent the rigid body motion of the element. Although the element motion is a rigid body motion, its internal deformations are represented by the spring deformation around each element. This means that although the element shape doesn't change during analysis, the behavior of assembly of elements is deformable. The two elements shown in Fig. (2) are assumed to be connected by only one pair of normal and shear springs. To have a general stiffness

matrix, the location of element and contact springs are assumed in a general position. The stiffness matrix components corresponding to each degree of freedom are determined by assuming a unit displacement in the studied direction and by determining forces at the centroid of each element. The element stiffness matrix size is only (6 x 6). Equation (2) shows the components of the upper left quarter of the stiffness matrix. All used notations in this equation are shown in Fig. (2). It is clear that the stiffness matrix depends on the contact spring stiffness and the spring location. The stiffness matrix in Eq. (2) is for only one pair of contact springs. However, the global stiffness matrix is determined by summing up the stiffness matrices of individual pair of springs around each element. Consequently, the developed stiffness matrix is an average stiffness matrix for the element according to the stress situation around the element. This technique can be used both in load and displacement control cases.

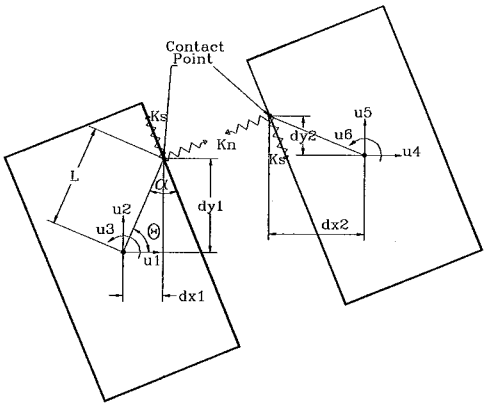

Fig. (2) Element shape, contact point and degrees of freedom

$$\begin{bmatrix} \sin^2(\theta+\alpha)K_n + \cos^2(\theta+\alpha)K_s & -K_n\sin(\theta+\alpha)\cos(\theta+\alpha) + K_s\sin(\theta+\alpha)\cos(\theta+\alpha) & \cos(\theta+\alpha)K_sL\sin(\alpha) - \sin(\theta+\alpha)K_nL\cos(\alpha) \\ -K_n\sin(\theta+\alpha)\cos(\theta+\alpha) + K_s\sin(\theta+\alpha)\cos(\theta+\alpha) & \sin^2(\theta+\alpha)K_s + \cos^2(\theta+\alpha)K_n & \cos(\theta+\alpha)K_nL\cos(\alpha) + \sin(\theta+\alpha)K_sL\sin(\alpha) \\ \cos(\theta+\alpha)K_sL\sin(\alpha) - \sin(\theta+\alpha)K_nL\cos(\alpha) & \cos(\theta+\alpha)K_nL\cos(\alpha) + \sin(\theta+\alpha)K_sL\sin(\alpha) & L^2\cos^2(\alpha)K_n + L^2\sin^2(\alpha)K_s \end{bmatrix} \quad (2)$$

NUMERICAL PROCEDURE TO CONSIDER LARGE DEFORMATION EFFECTS

The developed stiffness matrix in Eq. (1) is based on assumption that deformations are small. Special techniques should be used to consider the effects of geometrical changes of the structure. Two main factors should be considered to be able to extend the analysis to the large deformation zone:

1. Calculation of the stiffness matrix for the new structural geometry.
2. Redistribution of the internal forces due to geometrical changes.

In the FEM, these effects can be taken into account by adopting geometrical stiffness matrix[3]. In the proposed technique, we don't have to determine the geometrical stiffness matrix resulting in making the method general and easier in application without affecting the accuracy of the analysis. On the other hand, initial imperfection should be used to break the symmetry of structures. The main assumption in the formulation used is that the direction of the applied external forces is constant. Follower loading condition[3], which means that applied load direction changes when the member buckles, can not be analyzed using the proposed formulation. To develop the methodology for static large deformation analysis, the following steps are proposed. The general equation of motion under static loading is:

$$[K][\Delta U] = \Delta f + R_m + R_G \quad (3)$$

Where [K] is nonlinear stiffness matrix; Δf the incremental applied load vector and $[\Delta U]$ the incremental displacement vector. The term, R_m, is residual force vector due to cracking or incompatibility between strains and stresses at the spring location, while R_G is residual forces due to geometrical changes of the structure during loading. It should be emphasized that the stiffness matrix is calculated for the structure after applying the geometrical changes. Nonlinear material behavior is considered in determination of [K] and R_m. To calculate the residual forces due to geometrical changes, the following technique is proposed:

1. Assume that R_m and R_G are zeros and solve the equation to get incremental displacement, $[\Delta U]$. Solution can be performed under displacement or load control.
2. Modify the geometry of the structure according to the calculated incremental displacements. This indicates that the location of the contact points is also changed.

3. Modify the direction of spring force vectors according to the new element configuration. Incompatibility between applied forces and internal stresses occurs due to geometrical changes.
4. Check the situation of cracking, in case of nonlinear material, and calculate the material residuals load vector Rm. In elastic analysis, R_m equals zero.
5. Calculate the element force vector, F_m, from surrounding springs of each element.
6. Calculate the geometrical residuals around each element from the equation below.

$$R_G = f - F_m \tag{4}$$

Equation above means that the geometrical residuals account for the incompatibility between external applied forces, f, and internal forces, F_m, due to modification of geometry of the structure.

7. Calculate the stiffness matrix for the structure in the new configuration considering stiffness changes at each spring location due to cracking or yield of reinforcement, in case of nonlinear material.
8. Apply again a new load or displacement increment and repeat the whole procedure.

Residuals calculated from the previous increment can be incorporated in solution of Eq. (3) to reduce the time of calculation.

Although this technique is simple, the numerical results showed high accuracy in following the structural behavior. However, the following limitations should be noticed:

1. Complete symmetry of the structure and loading should be avoided during the large deformation analysis. The symmetry can be broken by, for example, making a slight change of one of material parameters of a part of the structure.
2. It should be emphasized that small deformation theory is assumed during each increment. This means that the load or displacement increments should be small enough to follow the geometrical changes.

In many applications, apparent stiffness of structure decreases after buckling and hence, the applied load should also decrease. In case of load-control analysis, assuming a positive value of load increment, cumulative difference between the applied loads and internal loads appears after buckling. Applying additional load increments after buckling results in divergence in the geometrical residual values and hence, large geometrical changes occur at little number of increments. In some cases, solution can not be continued because of divergence in the solution scheme. To overcome this problem, displacement control analysis is suggested. However, displacement control method is limited in application to cases where the load is applied at little number of points. The proposed technique can be modified easily to adopt energy method or arc length method[13] to follow such kind of problems. This problem disappears when load-control analysis is applied to the structure in dynamic way because the difference between applied loads and internal forces results in increasing the inertia force of structure and hence, equilibrium is maintained.

SIMULATION OF BUCKLING AND POST BUCKLING BEHAVIOR IN STATIC CONDITION

a) Fixed Base Cantilever

The first case study of buckling and post buckling behavior is performed using of a fixed base elastic cantilever under axial load. The load direction is assumed constant during analysis. The height of the cantilever is 12.0 m and the cross section is (1.0 m x 1.0 m). The Young's modulus assumed is 8.4×10^4 tf/m^2. The analysis is performed using 300 elements. The load is applied at the top of the column with the constant-rate vertical displacement. To break symmetry of the system, the stiffness of one of edge elements was increased by just 1% relative to the other elements. Analysis is performed under two conditions, with and without the consideration of geometrical residuals.

Figure (3) illustrates the deformed shape of the cantilever during and after buckling. It is obvious that highly nonlinear geometrical changes can be followed. Figure (4) shows the horizontal and vertical displacements at the loading point in three different cases with and without consideration of the geometrical residuals together with the theoretical load-displacement relations[1]. The theoretical results can be obtained by the following:

1. Assume the angle α (ranges between 0 and π).
2. Solve Eq. (5) below numerically and calculate the applied load. Where P is the applied load; E Young's modulus; I moment of inertia; L the cantilever length and Φ the integration parameter.

$$P = \frac{EI}{L^2}\left[\int_0^{\frac{\pi}{2}} \frac{d\Phi}{\sqrt{1-\sin^2\left(\frac{\alpha}{2}\right)\sin^2(\Phi)}}\right]^2 \tag{5}$$

$$DY = 2L - \frac{2}{\sqrt{\frac{P}{EI}}}\left[\int_0^{\frac{\pi}{2}} \sqrt{1-\sin^2\left(\frac{\alpha}{2}\right)}\sin^2(\Phi)d\Phi\right]^2 \tag{6}$$

3. Solve Eq. (6) numerically and calculate the vertical displacement "DY"
4. Calculate the horizontal displacement, DX, using Eq. (7).
5. Assume a new angle α and go to the step (2).

$$DX = \frac{2\sin\left(\frac{\alpha}{2}\right)}{\sqrt{\frac{P}{EI}}}\int_0^{\frac{\pi}{2}}\sin(\Phi)d\Phi = \frac{2\sin\left(\frac{\alpha}{2}\right)}{\sqrt{\frac{P}{EI}}} \tag{7}$$

In theoretical results, the effects of axial and shear deformations are neglected. Although these effects are relatively small, they are taken into account in our analysis. From Fig. (3) and Fig. (4) the following can be noticed:

1. The load-displacement relation obtained when the geometrical residuals are considered is close to the theoretical values till very large displacements. This gives evidence that the proposed method is accurate and numerically stable.
2. The calculated buckling load without consideration of geometrical residuals, only with modification of geometry, was about 47 tf which is quite larger than the theoretical one (7.8 tf). This means that modification of the geometry only during the analysis is not sufficient.
3. The calculated load-displacement relation is tangent to the horizontal line at the buckling load value which agrees well with the theory.
4. Slight increase in the load after buckling results in very large displacements. This indicates that applying load control technique after buckling leads to very large deformations during small number of increments. This causes numerical instability of the analysis after buckling.
5. When the vertical displacement is about 9 m, horizontal displacement begins to decrease.
6. The cantilever shape changes after buckling to an arch, which makes the stiffness of the specimen increase after buckling.

Figure (5) shows the load-stress relation of the point "A" under the applied load. Before buckling, stress is mainly compression and increases in a linear way. When reaching the buckling load, compression stresses are released till reaching zero when the direction of load becomes parallel to the cantilever end edge, stage (8) in Fig. (3). Finally, tension stresses develop and increase.

Changes in internal stresses of an intermediate section during analysis are shown in Fig. (6). Before buckling, stresses are mainly uniform compression and only axial deformations are observed. After reaching the buckling load, although the applied load is constant (P≈7.8 tf), bending moments generates and large deformation occurs because of the buckling bending moments. This shows one of the strong points in our analysis that mechanical behavior of any point in the structure can be followed accurately even if large deformations occur.

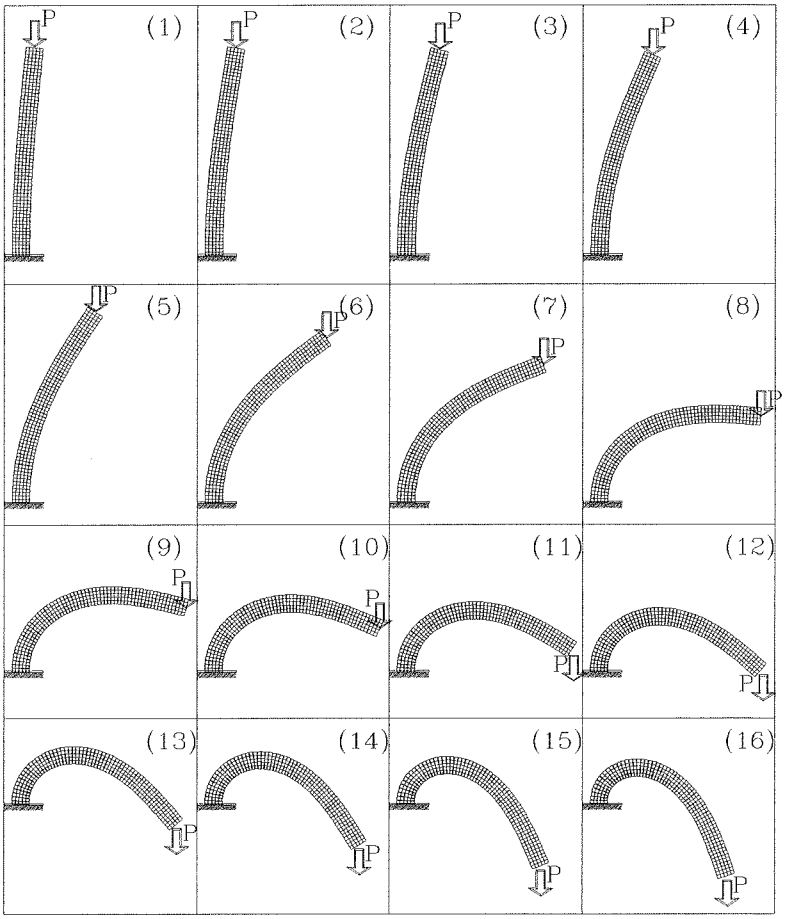

Fig. (3) Post buckling behavior of a cantilever

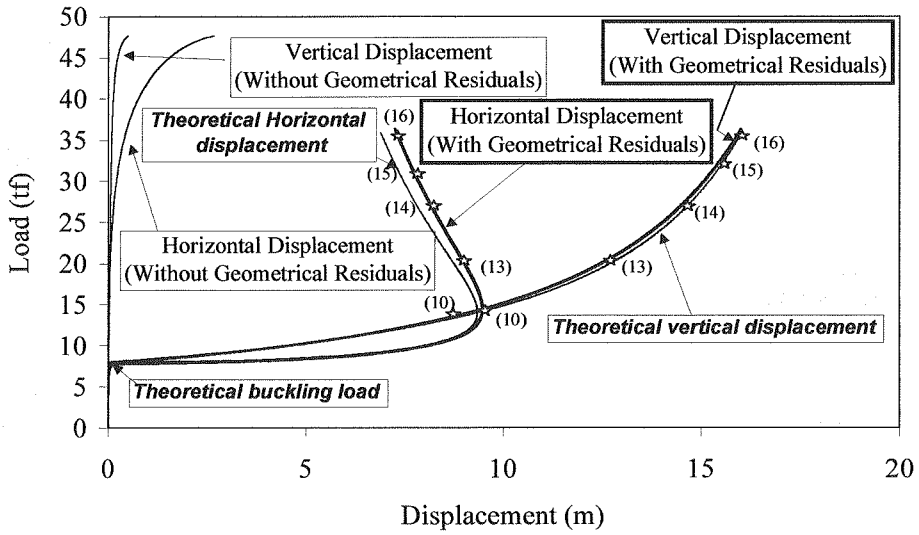

Fig. (4) Load-displacement relation of an elastic cantilever under vertical load

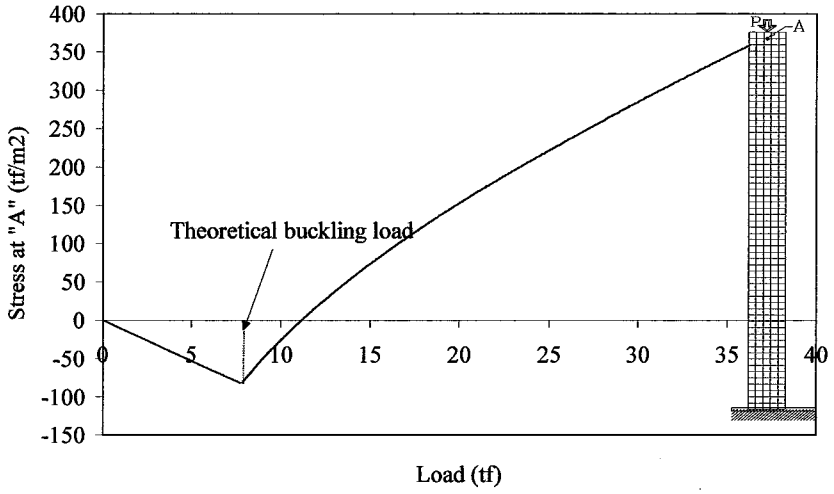

Fig. (5) Load-stress relation at point "A"

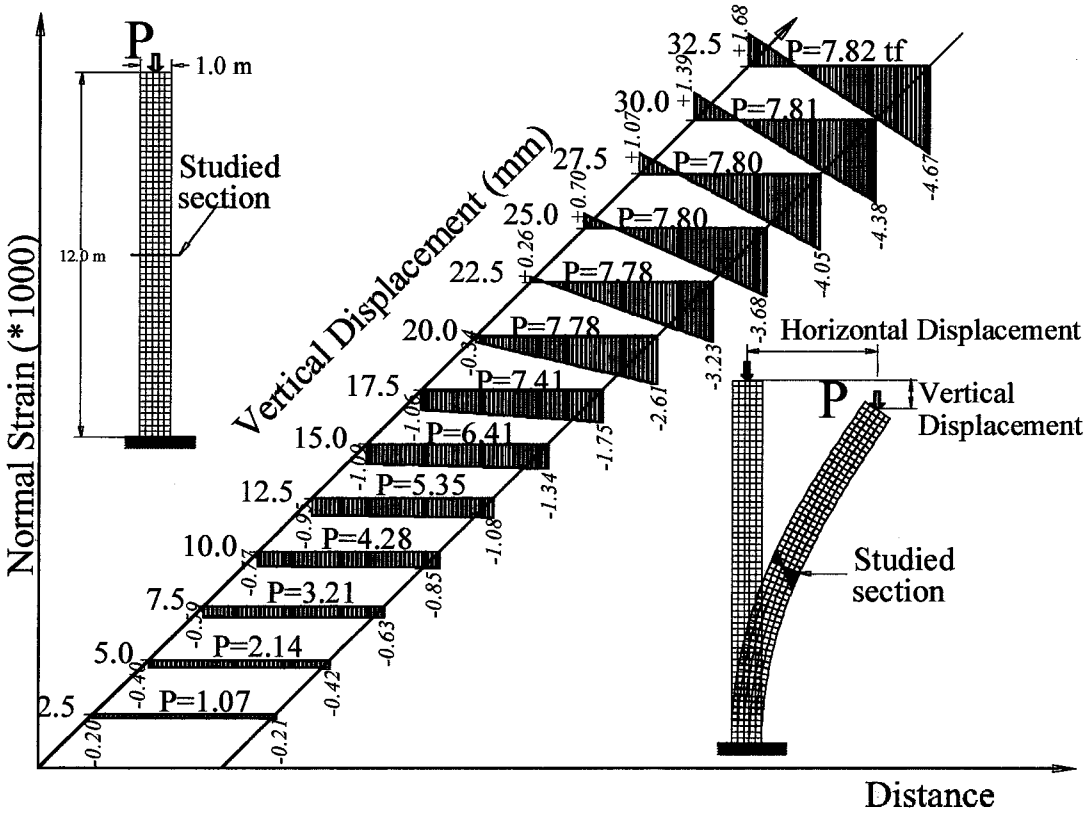

Fig. (6) Variation of internal stress distribution during buckling

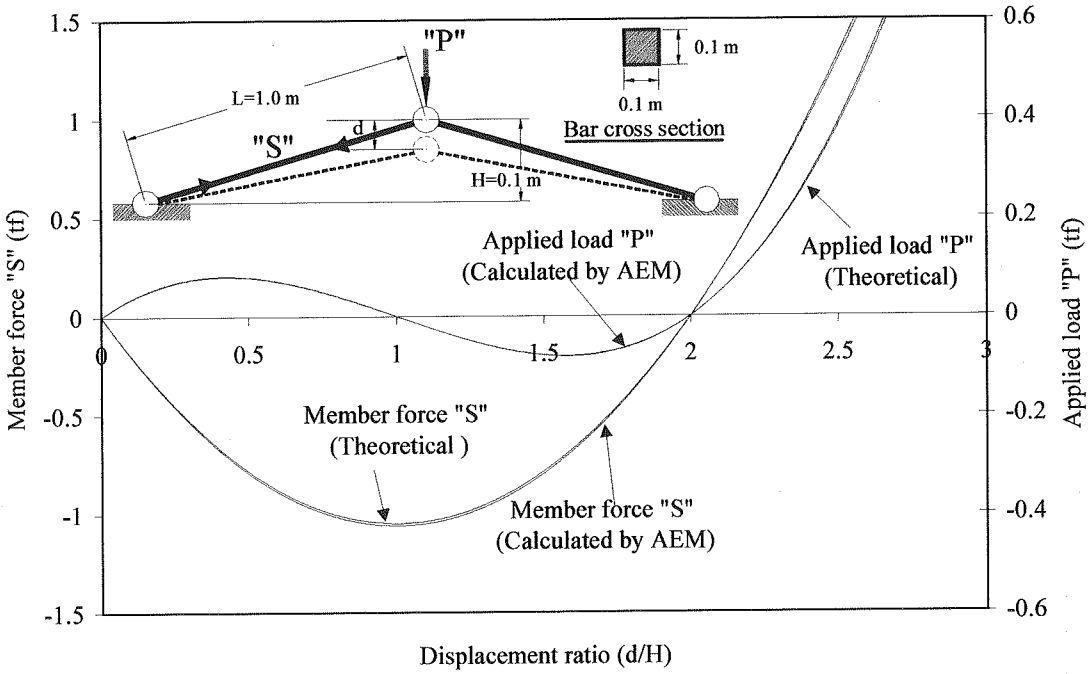

Fig. (7) Relations between applied load, member force and displacement ratio under vertical constant rate applied displacement condition

b) Snap Through Buckling of Two-Member Truss

The second case study is simulation of buckling behavior of two members truss[2]. The truss dimensions and loading point location is shown in Fig. (7). The truss cross section is (0.1 m x 0.1 m). The Young's modulus is assumed 2.1 x 10^4 t/m^2. Half of the truss is analyzed because of symmetry, using 11 square elements of size (0.1m x 0.1m). The load was applied at the intermediate hinge with the constant-rate displacement control. The load-displacement relation and the member force are shown in Fig. (7). The results of the load-displacement are compared with the theoretical ones. It takes only 1 minutes using a personal computer (CPU Pentium 267 MHz) to make such analysis. Almost no difference exists between the calculated and theoretical results. The theoretical relations between applied load, P, member force, S, and displacement, d, can be obtained simply from Eqs. (8) and (9).

$$S = \frac{EA}{L}\left(L - \sqrt{\left(L^2 - H^2\right) + (H-d)^2}\right) \tag{8}$$

$$P = 2S\frac{H-d}{\sqrt{\left(L^2 - H^2\right) + (H-d)^2}} \tag{9}$$

Parameters shown in Eqs (8) and (9) are shown in Fig. (7). The truss during deformation passes through the following stages:

1. Because the member length decreases during loading, compressive member force increases. The shortest member length, maximum member force, is achieved when the member becomes horizontal.
2. When the member is horizontal, compression force is maximum while the applied load value is zero since it is applied in vertical direction.
3. Increasing the displacements after horizontal position leads to increase the member length, and hence, compressive force is released. The direction of applied load is reversed.

4. When (d/H) value equals 2.0, the member length becomes the same as the initial value and hence, member force and applied load become zero.
5. Increasing the applied displacement leads to increasing the tension force in the members.

c) Elastic Frame with Different Support Conditions

The third case study is simulation of buckling behavior of elastic frames. The frames are solved under three different conditions:

1. Base supports of the frame are fixed and side sway is permitted.
2. Base supports of the frame are fixed and side sway is not permitted.
3. Base supports of the frame are hinged and side sway is permitted.

Two vertical loads are applied at corners. The frame dimensions and loading points location are shown in Fig. (8). The frame cross section is (0.5 m x 0.5 m). The Young's modulus is assumed 2.1 x 10^4 tf/m^2. The load is applied at the top of the column with the constant-rate load control. To break symmetry of the system, the stiffness of one of edge elements was increased by just 1 % relative to the other elements. This analysis can not be performed under displacement control because displacement of frame corners after buckling are different because of change in values of axial force in the columns. Making the analysis under load control necessitates that the applied load increment should be very small after buckling.

For the first case, analysis is performed using 136 elements. The results are shown in Fig. (8). The buckling load obtained is very close to the theoretical one[14]. After buckling, displacements increase drastically in few increments because the loading is applied under load control.

The results of the second case are shown in Fig. (9). Analysis is performed for half of the frame because of symmetry. As the load is applied at only one point, analysis can be performed under displacement control up to large displacements and the results are stable. The results are shown in Fig. (9). The buckling load when side sway is not permitted is much higher than when it is permitted. The theoretical buckling load value is not available for this case. However, buckling mode obtained, shown in Fig. (9), seems to be realistic. Analysis stops before the recontact of elements. This effect will be discussed in details in further publication.

Figure (10) show the results of the third case study. Analysis is performed using 306 elements under load control. Buckling load obtained is very close to the theoretical one[14] and its value is much less than when the frame base supports are fixed.

CONCLUSIONS

In this study, a new extension for the AEM was developed by which structure behavior can be simulated even when large geometrical changes occur. It was proved through numerical simulations that this technique has the following advantages:

1. The proposed technique is relatively simple compared to existing numerical techniques.
2. Through comparison with other numerical techniques, it was proved that this technique can follow the structural behavior accurately even in large deformation range where large geometrical changes are observed. The simulated buckling loads, buckling modes and internal stresses agree well with the theoretical results.
3. This technique is general and can be applied to any structure or material type.
4. This technique can be extended easily to follow large deformation of structures till total collapse. This is illustrated in other publications.

However, the following limitations in application exist:

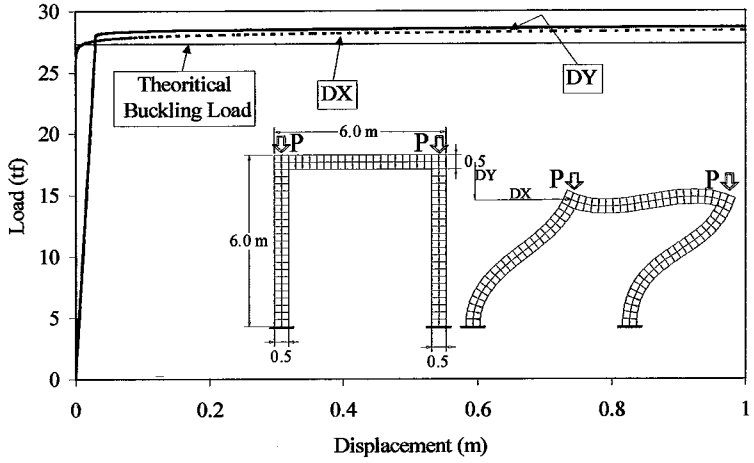

Fig. (8) Load-deformation relation of a fixed-fixed frame under vertical loads.(Side sway is permitted)

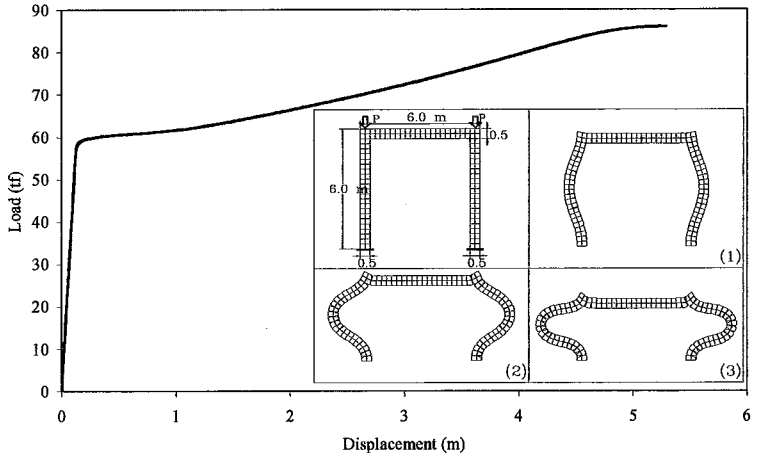

Fig. (9) Load-deformation relation of a fixed-fixed frame under vertical loads.(Side sway is not permitted)

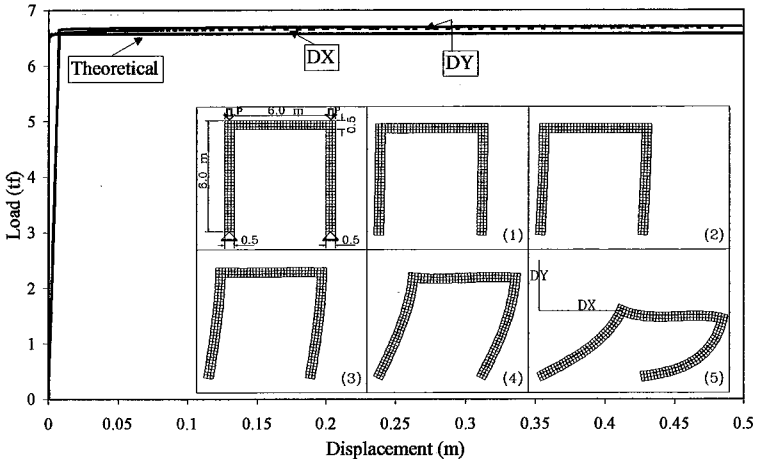

Fig. (10) Load-deformation relation of a hinged-hinged frame under vertical loads.

1. The load direction is assumed constant. Follower loading condition, which means that applied load direction changes when the member buckles, and non-conservative loads in general can not be studied using the proposed formulation.
2. Although the applied load condition can be adopted as load and displacement control, both of them have their own limitations. Load control can not follow post peak behavior while displacement control technique can not follow cases when the tangent to the load-deformation curve tends to be vertical[13]. In addition, displacement control technique can not be adopted to cases where load is applied at many points. However, the method can be extended easily to follow other methods of loading like energy control or arc length control methods[14].

REFERENCES

1. Farshad M.: Stability of structures , Elsevier Science Publishing Co. Inc., Amsterdam, 1994.
2. Szabo J., Gaspar Z. and Tarnai T.: Post-buckling of elastic structures, Elsevier Science Publishing Co. Inc., Budapest 1986.
3. Waszczyszyn Z., Cichon C. and Radwanska M.: Stability of structures by finite element methods, Elsevier Science Publishing Co. Inc., Amsterdam, 1994.
4. Meguro K. and Hakuno M.: Fracture analyses of structures by the modified distinct element method, Structural Eng./Earthquake Eng., Vol. 6. No. 2, 283s-294s., Japan Society of Civil Engineers, 1989.
5. Meguro K. and Hakuno M.: Application of the extended distinct element method for collapse simulation of a double-deck bridge, Structural Eng./Earthquake Eng., Vol. 10. No. 4, 175s-185s., Japan Society of Civil Engineers, 1994.
6. Kawai T.: Some considerations on the finite element method, Int. J. for Numerical Methods in Engineering, Vol. 16, pp. 81-120, 1980.
7. Kikuchi A., Kawai T. and Suzuki N.: The rigid bodies-spring models and their applications to three dimensional crack problems, Computers & Structures, Vol. 44, No. 1/2, pp. 469-480, 1992.
8. Amadei B., Lin C. and Dwyer J.: Recent extensions to the DDA method, Proc. of 1st Int. Forum on Discontinuous Deformation Analysis (DDA), Berkley, California, Ed. Salami & Banks (1996).
9. Meguro K. and Tagel-Din H.: A new efficient technique for fracture analysis of structures, Bulletin of Earthquake Resistant Structure, No. 30, pp. 103-116, 1997.
10. Tagel-Din H. and Meguro K.: Consideration of Poisson's ratio effect in structural analysis using elements with three degrees of freedom, Bulletin of Earthquake Resistant Structure, No. 31, pp. 41-50, 1998.
11. Meguro K. and Tagel-Din H.: A new simplified and efficient technique for fracture behavior analysis of concrete structures, Proceedings of the Third International Conference on Fracture Mechanics of Concrete and Concrete Structures (FRAMCOS-3), Gifu, Japan, Oct. 1998.
12. Meguro K. and Tagel-Din H.: A new simple and accurate technique for failure analysis of structures, Bulletin of Earthquake Resistant Structure, No. 31, pp. 51-61, 1998.
13. Kleiber M.: Incremental finite element modeling in non-linear solid mechanics, Ellis Horwood, New York, 1989.
14. Timoshinko S. and Gere J.: Theory of elastic stability, McGraw-Hill Inc., 1961.